Atmospheric Environment 224 (2020) 117349

Contents lists available at ScienceDirect

Atmospheric Environment

journal homepage: http://www.elsevier.com/locate/atmosenv

Comprehensive characterization of hygroscopic properties of methanesulfonates

Liya Guo [a,e,1], Chao Peng [a,1], Taomou Zong [b], Wenjun Gu [a,e], Qingxin Ma [c,e,f], Zhijun Wu [b], Zhe Wang [d], Xiang Ding [a], Min Hu [b], Xinming Wang [a,e,f], Mingjin Tang [a,e,f,*]

[a] State Key Laboratory of Organic Geochemistry and Guangdong Key Laboratory of Environmental Protection and Resources Utilization, Guangzhou Institute of Geochemistry, Chinese Academy of Sciences, Guangzhou, 510640, China
[b] State Key Joint Laboratory of Environmental Simulation and Pollution Control, College of Environmental Sciences and Engineering, Peking University, Beijing, 100871, China
[c] State Key Joint Laboratory of Environment Simulation and Pollution Control, Research Center for Eco-Environmental Sciences, Chinese Academy of Sciences, Beijing, 100085, China
[d] Division of Environment and Sustainability, The Hong Kong University of Science and Technology, Hong Kong, China
[e] University of Chinese Academy of Sciences, Beijing, 100049, China
[f] Center for Excellence in Regional Atmospheric Environment, Institute of Urban Environment, Chinese Academy of Sciences, Xiamen, 361021, China

HIGHLIGHTS

- Hygroscopic properties of three methanesulfonates were investigated using two techniques.
- The mass change of CH_3SO_3Na at 90% RH, relative to that at <1% RH, was measured to be ~4.0.
- The growth factor was measured to be 1.48 ± 0.02 at 90% RH for CH_3SO_3Na aerosol.

ARTICLE INFO

Keywords:
Hygroscopic properties
Methanesulfonate
Aerosol-water interaction
Dimethyl sulfide
Marine aerosol

ABSTRACT

Methanesulfonate, formed in atmospheric oxidation of dimethyl sulfide, is abundant in marine aerosols; however, its hygroscopic properties have not been well understood. In this work, two complementary techniques (a vapor sorption analyzer and a humidity tandem differential mobility analyzer) were employed to investigate hygroscopic properties of CH_3SO_3Na, CH_3SO_3K and $(CH_3SO_3)_2Ca$ at different relative humidities (RH). The deliquescence relative humidities were measured to be 70–71% for CH_3SO_3Na at 15–35 °C, displaying no dependence on temperature. The mass changes at 90% RH, relative to that at <1% RH, were measured to be 4.002 ± 0.053 for CH_3SO_3Na, 3.479 ± 0.031 for CH_3SO_3K, and 3.663 ± 0.019 for $(CH_3SO_3)_2Ca$ at 25 °C. CH_3SO_3Na and CH_3SO_3K aerosols started to grow at >70% RH, while continuous growth since very low RH (<40%) was observed for $(CH_3SO_3)_2Ca$ aerosols. At room temperature, hygroscopic growth factors at 90% RH were measured to be 1.48 ± 0.02, 1.53 ± 0.04 and 1.65 ± 0.02 for CH_3SO_3Na, CH_3SO_3K and $(CH_3SO_3)_2Ca$ aerosols, respectively.

1. Introduction

Dimethyl sulfide (DMS), one of the most abundant sulfur compounds in the troposphere, contributes ~50% of the biogenic emission of sulfur on the global scale (Andreae, 1990; Bates et al., 1994; Barnes et al., 2006). DMS is mainly produced by phytoplankton in sea surface water (Charlson et al., 1987), and after emitted into the atmosphere, it will be oxidized by atmospheric oxidants (OH, NO_3, O_3, and etc.), eventually leading to the formation of methanesulfonic acid (MSA) and sulfate. Once formed, MSA will partition into the particle phase and form methanesulfonate via homogeneous nucleation, condensation and heterogeneous reactions (Debruyn et al., 1994; Hanson, 2005; Tang and

* Corresponding author. State Key Laboratory of Organic Geochemistry and Guangdong Key Laboratory of Environmental Protection and Resources Utilization, Guangzhou Institute of Geochemistry, Chinese Academy of Sciences, Guangzhou, 510640, China.
E-mail address: mingjintang@gig.ac.cn (M. Tang).
[1] The two authors contributed equally to this work.

https://doi.org/10.1016/j.atmosenv.2020.117349
Received 30 September 2019; Received in revised form 3 February 2020; Accepted 14 February 2020
Available online 22 February 2020

Zhu, 2008; Tang et al., 2010; Dawson et al., 2012; Chen et al., 2016; Zhao et al., 2017).

Methanesulfonate has been identified at various locations in the world (Bates et al., 1992; Davis et al., 1999; Bardouki et al., 2003; Zorn et al., 2008; Lin et al., 2012; Ovadnevaite et al., 2014; van Pinxteren et al., 2015; Huang et al., 2017). For example, Ovadnevaite et al. (2014) measured chemical compositions of submicron aerosols at Mace Head (Ireland) from January 2009 to June 2011, and methanesulfonate concentrations and mass ratios of methanesulfonate to non-sea-salt sulfate were in the range of 0–0.09 μg m^{-3} and 0.04–0.46. In a campaign during June to July 2011, methanesulfonate concentrations were determined to be 18.8–65.1 ng m^{-3} over the tropical Atlantic Ocean, and the average mass ratio of methanesulfonate to non-sea-salt sulfate was found to be 0.022 (van Pinxteren et al., 2015). Huang et al. (2017) investigated latitudinal and seasonal variation of methanesulfonate over the Atlantic, and methanesulfonate concentrations and mass ratios of methanesulfonate to non-sea-salt sulfate were measured to be 0.01–0.03 μg m^{-3} and 0.007–0.173. To our knowledge, methanesulfonate is formed in the troposphere dominantly from DMS oxidation (Gondwe et al., 2004; Barnes et al., 2006; Sorooshian et al., 2015), and the ratio of methanesulfonate to non-sea-salt sulfate is often used to estimate the contribution of DMS to non-sea-salt sulfate aerosol. However, recent studies suggested that methanesulfonate would undergo rapid degradation due to heterogeneous oxidation by OH radicals (Kwong et al., 2018; Mungall et al., 2018).

Methanesulfonate, as an important component of aerosol particles in marine and coastal regions, can affect the climate directly by scattering solar radiation and indirectly by serving as cloud condensation nuclei (CCN) (Hodshire et al., 2019). The direct and the indirect radiative forcing both depend on aerosol hygroscopicity (Haywood and Boucher, 2000; Kanakidou et al., 2005; Tang et al., 2016; Bertram et al., 2018), and a few previous studies (Peng and Chan, 2001; Liu and Laskin, 2009; Zeng et al., 2014) have investigated hygroscopic properties of methanesulfonates. For example, Peng and Chan (2001) measured mass changes of levitated CH_3SO_3Na particles at 25 °C using an electrodynamic balance. The deliquescence relative humidity (DRH) and efflorescence relative humidity (ERH) were determined to be 65.2–68.9% and 50.1–51.1%; in addition, the ratio of particle mass at 90% RH to that under dry conditions was measured to be 4.22. Liu and Laskin (2009) employed microscopic Fourier transform infrared spectroscopy (micro-FTIR) to investigate hygroscopic properties of several methanesulfonates at 24 °C. They found that CH_3SO_3Na particles displayed distinctive phase transitions, and DRH and ERH were measured to be 71% and ~49%; in contrast, $CH_3SO_3NH_4$, $(CH_3SO_3)_2Mg$ and $(CH_3SO_3)_2Ca$ particles showed continuous hygroscopic behaviors without obvious phase transitions. Zeng et al. (2014) used an attenuated total reflection Fourier transform infrared spectroscopy (ATR-FTIR) to examine the temperature dependence of DRH and ERH of CH_3SO_3Na particles. DRH was found to increase from 71–73% at 23 °C to 82–84% at −5 °C, and ERH increased from 50–52% at 23 °C to 63–65% at −5 °C. In addition, hygroscopic properties of CH_3SO_3Na/NaCl internally mixed particles were also studied (Liu et al., 2011). Very recently, CCN activities of CH_3SO_3Na, CH_3SO_3K and $(CH_3SO_3)_2Ca$ aerosols were explored (Tang et al., 2015, 2019c). To our knowledge, hygroscopic properties of methanesulfonate aerosols have not yet been investigated.

In order to improve our knowledge in hygroscopic properties of methanesulfonate and thus its roles in the climate system, hygroscopic properties of three methanesulfonates, including CH_3SO_3Na, CH_3SO_3K and $(CH_3SO_3)_2Ca$, were investigated in this study using two complementary methods. A vapor sorption analyzer (VSA) was used to measure mass changes of the three methanesulfonates as a function of RH; furthermore, a humidity tandem differential mobility analyzer (H-TDMA) was employed to measure mobility diameters of submicron aerosol particles for the three methanesulfonates at different RH. The comprehensive dataset obtained in this work would improve our knowledge in hygroscopic properties of methanesulfonates, therefore helping us better understand the climatic effects of methanesulfonate aerosol and dimethyl sulfide.

2. Material and methods

NaCl (>99.5%) was purchased from Sigma-Aldrich, and artificial inorganic sea salt (its composition can be found in Table 1) was purchased from HIMEDIA. CH_3SO_3Na (>98%) and CH_3SO_3K (>99%) were both supplied by Alfa Aesar, and $(CH_3SO_3)_2Ca$ (>98.0%) was provided by Tokyo Chemical Industry (TCI). All the chemicals were used without further purification.

2.1. Vapor sorption analyzer experiments

A vapor sorption analyzer (VSA, Q5000SA), purchased from TA Instruments (New Castle, DE, USA), was employed to measure mass changes of methanesulfonate samples as a function of RH under isotherm conditions. The instrument was detailed elsewhere (Gu et al., 2017b; Tang et al., 2019b), and therefore is only described here in brief. Experiments were conducted at 15–35 °C (with an accuracy of ±0.1 °C) and 0–90% RH (with an absolute accuracy of ±1%). A high precision balance was used to measure the bulk sample mass, and the sensitivity was stated to be <0.1 μg. The balance had a dynamic range of 0–100 mg, and the sample mass under dry conditions (<1% RH) was typically in the range of 0.2–1.0 mg.

Mass growth factors of methanesulfonates were determined using the following procedure: i) at a given temperature, the sample was dried at <1% RH; ii) RH was increased to 90% stepwise with an increment of 5% per step; iii) after that, RH was returned to <1% to dry the sample again. To measure the DRH at a given temperature, the sample was dried at <1% RH, and after that RH was increased to a value which was at least 5% lower than the expected DRH; RH was then increased stepwise with an increment of 1% per step until a significant increase in sample mass was observed (i.e. the sample was deliquesced). In all the experiments, RH was changed to the next value only when the sample reached an equilibrium with the environment, and the sample was considered to reach an equilibrium when its mass change was <0.1% within 30 min. All the experiments were conducted in triplicate.

2.2. H-TDMA experiments

A humidity tandem differential mobility analyzer (H-TDMA), developed at Peking University, was used to investigate hygroscopic growth of methanesulfonate aerosol particles at 25 ± 1 °C via measuring mobility diameters of quasi-monodisperse aerosol particles at different RH. The H-TDMA used in our work was described elsewhere (Wu et al., 2011, 2017). In brief, an atomizer was used to generate polydisperse aerosol particles from aqueous solutions (around 0.4 g/L in water), and the aerosol flow was passed through a Nafion dryer to reduce its RH to <30%. After that, a dry aerosol flow (1 L min^{-1}) was delivered through an aerosol neutralizer and then the first differential mobility analyzer to

Table 1
Composition of artificial sea salt used in this study.

element	concentration (mg/L)
chloride (Cl)	38000
sodium	10780
sulfate	2660
potassium	420
calcium	400
carbonate (bicarbonate)	200
strontium	56
iodide	0.24
fluoride	1
magnesium (Mg)	1320
other trace elements	<0.5

select quasi-monodisperse aerosol particles with a dry diameter of 100 nm. Finally, the aerosol flow entered a humidification system (the residence time: ~2.5 s) to be humidified to a given RH, and the aerosol number size distribution was measured using the second DMA coupled to a condensation particle counter (CPC, TSI 3772). The flow rate ratio of the sheath flow to the aerosol flow was set to 10:1 for both DMA, and the total absolute uncertainty in RH was estimated to be <2%.

Some experiments were also carried out using the second H-TDMA developed at Research Center for Eco-Environmental Sciences, Chinese Academy of Sciences, and more information of this instrument can be found in a recent study (Ma et al., 2019).

3. Results and discussion

3.1. Mass change of methanesulfonates at different RH

3.1.1. DRH of CH_3SO_3Na particles

Fig. 1b displays changes in RH and normalized sample mass as a function of time in an experiment to measure the DRH of CH_3SO_3Na. When RH increased from 70% to 71%, a large increase in sample mass occurred, suggesting that the DRH of CH_3SO_3Na at 25 °C was 70.5 ± 0.5%. The small increase in sample mass, observed when RH increased from 69% to 70%, was very likely due to signal noise and/or baseline drifts. Peng and Chan (2001) employed an electrodynamic balance to study hygroscopic properties of CH_3SO_3Na particles at 25 °C, and the DRH was measured to be 65.2–68.9%. In another two studies, the DRH of CH_3SO_3Na was determined to be ~71% at 24 °C (Liu and Laskin, 2009) and 71–73% at 23 °C (Zeng et al., 2014). As a result, DRH measured in our work at around room temperature agreed very well with those reported by Liu and Laskin (2009) and Zeng et al. (2014), but was slightly higher than that reported by Peng and Chan (2001).

We also investigated the DRH of CH_3SO_3Na at different temperatures, and found that it showed no significant variation with temperature in the range of 15–35 °C. The lowest temperature our VSA could reach was 15 °C, though experiments at lower temperature (for example, below 0 °C) will be very valuable. In a previous study, Zeng et al. (2014) measured the DRH of CH_3SO_3Na particles at different temperature, and the DRH at 12 °C was determined to be ~74%, in reasonably good agreement with our work (~71% at 15 °C). Zeng et al. suggested that DRH of CH_3SO_3Na showed a negative temperature dependence, increasing from 71–73% at 23 °C to 82–84% at −5 °C, while no significant temperature dependence (15–35 °C) was found in our work.

3.1.2. Mass hygroscopic growth of methanesulfonates

Fig. 1a displays a typical experiment conducted to measure mass hygroscopic growth factors of CH_3SO_3Na at 25 °C. Significant increase in sample mass was observed when RH was changed from 70% to 75%; this suggested that the deliquescence of CH_3SO_3Na took place at 70–75% RH, being consistent with the measured DRH (70–71%). As shown in Fig. 1a, further increase in RH resulted in additional increase in sample mass.

Fig. 2 shows mass growth factors (defined as the ratio of sample mass at a given RH to that at <1% RH) of CH_3SO_3Na, CH_3SO_3K and $(CH_3SO_3)_2Ca$ particles at 25 °C in the RH range of 0–90%, and the data are also summarized in Table 2. The measured mass growth factor of CH_3SO_3Na has a very large error at 70% RH. As discussed in Section

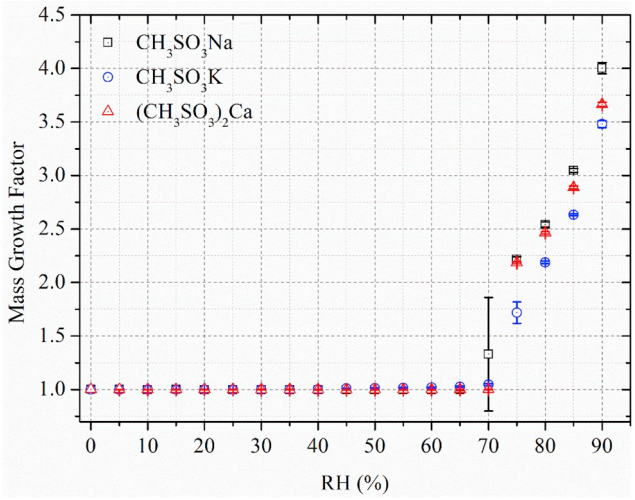

Fig. 2. Mass growth factors of three methanesulfonates as a function of RH at 25 °C.

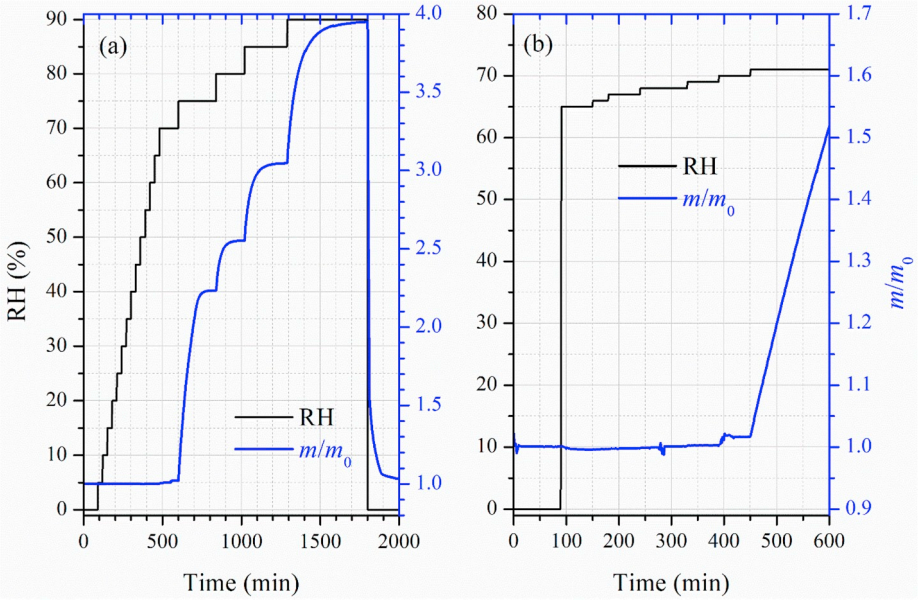

Fig. 1. Normalized sample mass of CH_3SO_3Na (relative to the dry mass, blue curve, right y axis) and RH (black curve, left y axis) as a function of time at 25 °C. (a) A typical experiment conducted to measure mass hygroscopic growth factors; (b) a typical experiment conducted to measure the DRH. (For interpretation of the references to colour in this figure legend, the reader is referred to the Web version of this article.)

3.1.1, the DRH of CH_3SO_3Na was measured to be 70–71%; therefore, at 70% RH CH_3SO_3Na may remain as solid in one experiment while deliquesce to form an aqueous solution in another experiment, leading to large uncertainties in the measured mass growth factors. As shown in Fig. 2, CH_3SO_3K and $(CH_3SO_3)_2Ca$ also deliquesced when RH increased from 70% to 75%. The mass growth factors at 90% RH were determined to be around 4.00, 3.48 and 3.66 for CH_3SO_3Na, CH_3SO_3K and $(CH_3SO_3)_2Ca$, respectively.

For deliquesced samples, we also calculated their water to solute ratios (WSR), defined as the molar ratio of H_2O to $CH_3SO_3^-$, and the results are displayed in Fig. 3 and Table 2. At around room temperature, WSR at 90% RH were determined to be 19.7 ± 0.3, 18.5 ± 0.2 and 17.0 ± 0.1 for CH_3SO_3Na, CH_3SO_3K, and $(CH_3SO_3)_2Ca$. WSR were measured to be 8.74 and 10.7 at 75% and 80% RH for CH_3SO_3Na in one previous study (Liu and Laskin, 2009), and 8.25, 10.69, 14.39 and 21.11 at 75%, 80%, 85% and 90% RH in another study (Peng and Chan, 2001). For comparison, in our work WSR were found to be 8.0 ± 0.1, 10.1 ± 0.1, 13.4 ± 0.1 and 19.7 ± 0.3 at 75%, 80%, 85% and 90% RH for CH_3SO_3Na. Overall, the agreement between our work and the two previous studies was very good, and the differences in WSR did not exceed 10%. For $(CH_3SO_3)_2Ca$, WSR were measured to be 13.11 and 16.13 at 75% and 80% by Liu and Laskin (2009); for comparison, WSR in our work were determined to be 7.6 ± 0.1 and 9.4 ± 0.1 at 75% and 80% RH, significantly smaller than those reported by Liu and Laskin (2009).

Several previous studies (Liu and Laskin, 2009; Gu et al., 2017a; Jia et al., 2018) suggested that WSR of deliquesced particles can be fitted by polynomial equations. As shown in Fig. 3, we also found that Eq. (1) could well fit the WSR data for CH_3SO_3Na, CH_3SO_3K and $(CH_3SO_3)_2Ca$, and the corresponding polynomial coefficients obtained are listed in Table 3.

$$\mathrm{WSR} = k_0 + k_1 RH + k_2 RH^2 + k_3 RH^3 \quad (1)$$

Table 2
Mass growth factors (m/m_0) and water-to-solute ratios (WSR) as a function of RH (0–90%) at 25 °C for CH_3SO_3Na, CH_3SO_3K and $(CH_3SO_3)_2Ca$. All the errors given in this work are standard deviations.

RH (%)	CH_3SO_3Na		CH_3SO_3K		$(CH_3SO_3)_2Ca$	
	m/m_0	WSR	m/m_0	WSR	m/m_0	WSR
<1	1.000 ± 0.001		1.000 ± 0.001		1.000 ± 0.001	
5	1.000 ± 0.001		1.000 ± 0.001		1.000 ± 0.001	
10	0.999 ± 0.001		1.000 ± 0.001		1.000 ± 0.001	
15	1.000 ± 0.001		1.000 ± 0.001		1.000 ± 0.001	
20	1.000 ± 0.002		1.000 ± 0.001		1.000 ± 0.001	
25	0.999 ± 0.002		1.000 ± 0.001		1.000 ± 0.001	
30	0.999 ± 0.002		1.000 ± 0.001		1.000 ± 0.001	
35	0.999 ± 0.002		1.000 ± 0.001		1.000 ± 0.001	
40	0.999 ± 0.002		1.001 ± 0.001		1.000 ± 0.001	
45	0.999 ± 0.003		1.010 ± 0.002		1.000 ± 0.001	
50	0.998 ± 0.003		1.013 ± 0.003		1.000 ± 0.001	
55	0.999 ± 0.004		1.015 ± 0.004		1.000 ± 0.001	
60	0.998 ± 0.004		1.019 ± 0.005		0.999 ± 0.001	
65	0.998 ± 0.004		1.026 ± 0.006		1.000 ± 0.001	
70	1.330 ± 0.531		1.045 ± 0.011		1.000 ± 0.001	
75	2.217 ± 0.024	8.0 ± 0.1	1.718 ± 0.100	5.4 ± 0.3	2.185 ± 0.009	7.6 ± 0.1
80	2.541 ± 0.024	10.1 ± 0.1	2.189 ± 0.011	8.8 ± 0.1	2.464 ± 0.011	9.4 ± 0.1
85	3.046 ± 0.017	13.4 ± 0.1	2.634 ± 0.010	12.2 ± 0.1	2.888 ± 0.013	12.1 ± 0.1
90	4.002 ± 0.053	19.7 ± 0.3	3.479 ± 0.031	18.5 ± 0.2	3.663 ± 0.019	17.0 ± 0.1

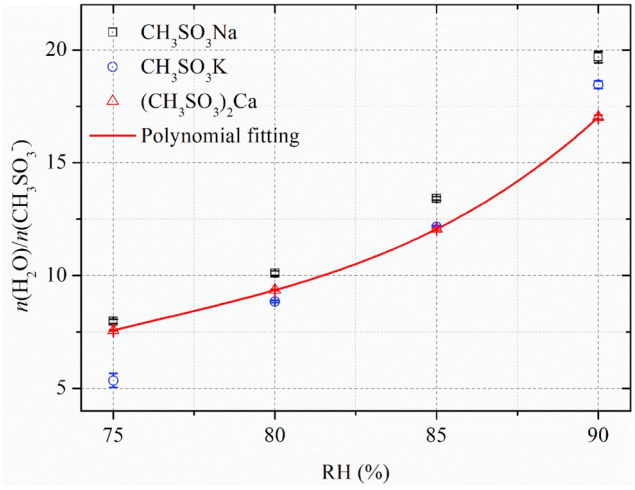

Fig. 3. Molar ratios of H_2O to $CH_3SO_3^-$ (WSR), $n(H_2O)/n(CH_3SO_3^-)$, as a function of RH for CH_3SO_3Na, CH_3SO_3K and $(CH_3SO_3)_2Ca$ at 25 °C. For clarity the fitting using Eq. (1) is only shown for $(CH_3SO_3)_2Ca$.

3.2. Hygroscopic growth of methanesulfonate aerosols

3.2.1. Hygroscopic growth of NaCl and sea salt aerosols

Fig. 4 shows hygroscopic growth factors of NaCl and sea salt aerosols at different RH (30–90%), measured using H-TDMA. Please note that a shape factor of 1.08 was applied to correct dry diameters of both aerosols (Kelly and McMurry, 1992; Fuentes et al., 2010). It can be concluded from Fig. 4 that our measured growth factors agreed very well with those predicted using E-AIM (Wexler and Clegg, 2002) for NaCl, suggesting that our H-TDMA measurements were robust.

In addition, hygroscopic growth factors of inorganic sea salt aerosols were measured. As displayed in Fig. 4, at a given RH above 75%, growth factors of sea salt aerosol were always slightly smaller than NaCl. Zieger et al. (2017) investigated hygroscopic properties of NaCl and sea salt aerosols, and reached a similar conclusion. The lower hygroscopicity of sea salt, when compared to NaCl, was caused by the fact that in addition to NaCl, sea salt also contains other compounds (such as $CaCl_2$ and $MgCl_2$), hygroscopicity of which was lower than NaCl (Gupta et al., 2015; Zieger et al., 2017; Bertram et al., 2018; Guo et al., 2019). An unknown technical problem occurred when we investigated hygroscopic growth of NaCl and sea salt aerosols, causing RH to be unstable at 50–70% RH; therefore, we did not measure their growth factors at 50–70% RH.

3.2.2. Hygroscopic growth of methanesulfonate aerosols

Hygroscopic growth factors of CH_3SO_3Na, CH_3SO_3K, and $(CH_3SO_3)_2Ca$ aerosols are displayed as a function of RH in Fig. 5 and Table 4. CH_3SO_3Na aerosol particles started to grow at 70% RH, and

Table 3
Polynomial coefficients obtained in this work when using Eq. (1) to fit WSR data for CH_3SO_3Na, CH_3SO_3K and $(CH_3SO_3)_2Ca$.

Particle	k_0	k_1	k_2	k_3	valid RH range
CH_3SO_3Na	−1093.042	42.288	−0.5461	0.00237	75–90%
CH_3SO_3K	−2222.275	82.218	−1.0168	0.00422	75–90%
$(CH_3SO_3)_2Ca$	−812.365	31.474	−0.4067	0.00177	75–90%

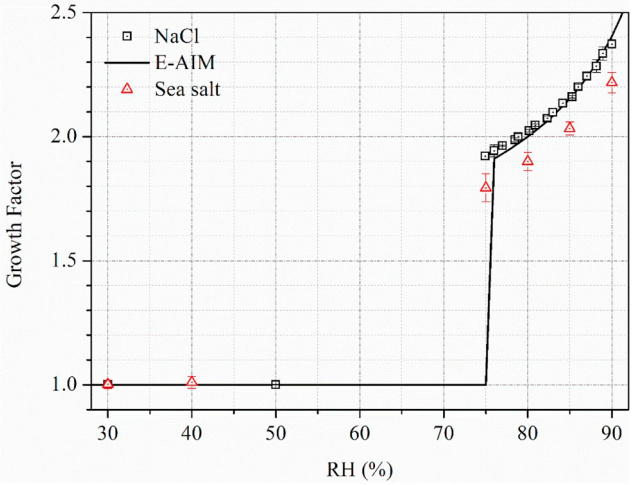

Fig. 4. Hygroscopic growth factors of NaCl and inorganic sea salt aerosols measured in this work. The black solid line represents growth factors of NaCl predicted using E-AIM.

growth factors were measured to be 1.12 ± 0.03, 1.28 ± 0.01 and 1.48 ± 0.02 at 70%, 80%, and 90%. Similarly, CH_3SO_3K aerosol particles started to grow at 75% RH, and growth factors were determined to be 1.20 ± 0.04, 1.31 ± 0.03 and 1.53 ± 0.04 at 75%, 80% and 90% RH. This is consistent with the observation (as presented in Section 3.1) that the mass of CH_3SO_3Na and CH_3SO_3K samples started to increase significantly at 70–75% RH due to onset of deliquescence.

Being different to CH_3SO_3Na and CH_3SO_3K, $(CH_3SO_3)_2Ca$ aerosols showed continuous hygroscopic growth, with growth factors being measured to be 1.08 ± 0.01 at 40% RH, 1.21 ± 0.01 at 60% RH, 1.43 ± 0.01 at 80% RH and 1.65 ± 0.02 at 90% RH. Continuous growth of aerosol particles has also been observed for other Ca- and Mg-containing salts (Gibson et al., 2006; Gupta et al., 2015; Jing et al., 2018; Guo et al., 2019), and this can be attributed to their amorphous state under dry conditions. In a previous study (Liu and Laskin, 2009), $(CH_3SO_3)_2Ca$ aerosol particles were generated and deposited on electron microscopy grids, and hygroscopic properties of these particles were then investigated using micro FTIR. $(CH_3SO_3)_2Ca$ particles examined by Liu and Laskin (2009) were very likely to be amorphous, and hence also exhibited continuous growth. Our VSA experiments found that no significant increase in sample mass was observed for $(CH_3SO_3)_2Ca$ at <75% RH. As the Kelvin effect was negligible for hygroscopic growth of 100

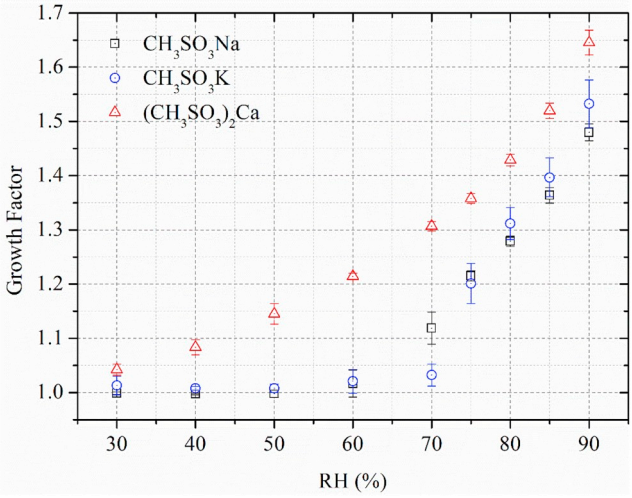

Fig. 5. Hygroscopic growth factors of CH_3SO_3Na, CH_3SO_3K and $(CH_3SO_3)_2Ca$ aerosol at different RH.

Table 4
Hygroscopic growth factors of CH_3SO_3Na, CH_3SO_3K, and $(CH_3SO_3)_2Ca$ aerosols at different RH.

RH (%)	CH_3SO_3Na	CH_3SO_3K	$(CH_3SO_3)_2Ca$
30	1.00 ± 0.01	1.01 ± 0.02	1.04 ± 0.01
40	1.00 ± 0.01	1.01 ± 0.01	1.08 ± 0.01
50	1.00 ± 0.01	1.01 ± 0.01	1.15 ± 0.02
60	1.02 ± 0.03	1.02 ± 0.02	1.21 ± 0.01
70	1.12 ± 0.03	1.03 ± 0.02	1.31 ± 0.01
75	1.22 ± 0.01	1.20 ± 0.04	1.36 ± 0.01
80	1.28 ± 0.01	1.31 ± 0.03	1.43 ± 0.01
85	1.36 ± 0.01	1.40 ± 0.04	1.52 ± 0.01
90	1.48 ± 0.02	1.53 ± 0.04	1.65 ± 0.02

nm aerosol particles (Tang et al., 2016), difference in sizes of particles used in the two types of experiments was not expected to play a significant role in the observed difference of deliquescence behaviors, and this was because $(CH_3SO_3)_2Ca$ samples used in our VSA experiments were likely to be crystalline and thus exhibited clear phase transitions during humidification.

3.3. Comparison of hygroscopicity derived from different methods

If it is assumed that the volume of a particle at a given RH is equal to the sum of the volume of water associated with the particle and the volume of the dry particle, mass change (measured in our work using VSA) can be converted to growth factors:

$$GF = \sqrt[3]{1 + V_w/V_0} = \sqrt[3]{1 + (\frac{m}{m_0} - 1)\cdot\frac{\rho_0}{\rho_w}} \quad (2)$$

where V_w is the volume of water associated with a particle at a given RH, V_0 is the volume of the dry particle, m and m_0 are the particle mass at the given RH and under dry conditions, and ρ_0 and ρ_w are the density of the dry particle and water. Particle sphericity assumption is also needed in order to derive Eq. (2). The density of CH_3SO_3Na was determined to be 1.955 g cm^{-3} (Tang et al., 2019c), and in the present work m/m_0 was measured to be 4.002 ± 0.053 at 90% RH for CH_3SO_3Na. As a result, growth factors derived from VSA measurements were 1.89–1.91 at 90% RH, significantly larger than that measured using H-TDMA (1.48 ± 0.02). Because such a large difference existed between VSA and H-TDMA results, we employed the second H-TDMA (Ma et al., 2019) to investigate hygroscopic growth of CH_3SO_3Na aerosol particles. The growth factors at 90% RH were measured to be 1.49 for 100 nm particles and 1.59 for 300 nm particles, in good agreement with that measured using the first H-TDMA. Therefore, growth factors measured in our work using H-TDMAs should be reliable. On the other hand, WSR data of CH_3SO_3Na particles derived from our VSA measurements agreed well with two previous studies (Peng and Chan, 2001; Liu and Laskin, 2009) and must also be robust. Additional studies which use H-TDMA, microscopic methods and/or optical tweezers to measure diameters of CH_3SO_3Na particles at different RH will be very useful to further validate our results.

The observed discrepancy between VSA and H-TDMA results may be due to the following factors. First of all, the underlying assumption used in Eq. (2) to convert mass change to diameter change, i.e. the volume of a particle at a given RH is equal to the sum of the volume of water associated with the particle and the dry particle volume, may not be valid for CH_3SO_3Na. Second, particles with different states were investigated using these two techniques; to be more specific, VSA examined particles contained in crucibles, while aerosol particles were studied using H-TDMA. Interactions between particles and substrates used to support these particles may result in differences in measured hygroscopicity (Eom et al., 2014; Tang et al., 2019a). Furthermore, supermicrometer and submicrometer particles were examined using VSA and H-TDMA, and the difference in particle sizes may also contribute to the observed difference in hygroscopicity. For example, a previous study

(Laskina et al., 2015) investigated hygroscopic properties of 100 nm aerosol particles (using H-TDMA) and ~6 μm particles (using micro-Raman spectroscopy), and found that hygroscopic properties of some inorganic/organic mixed particles depended on particle size.

The single hygroscopicity parameter (κ), widely used to describe aerosol hygroscopicity under both sub- and super-saturated conditions (Petters and Kreidenweis, 2007), can be calculated from H-TDMA measured growth factors, using Eq. (3):

$$\kappa_{gf} = (GF^3 - 1)\frac{1 - RH}{RH} \quad (3)$$

where κ_{gf} is the κ value derived from the measured growth factor (GF) at a given RH, and in our work growth factors measured at 90% RH were used to derive κ_{gf}. For CH_3SO_3Na aerosol, the average growth factor was measured to be 1.48 ± 0.02, and thus κ_{gf} was determined to be 0.24–0.26, which was significantly smaller than the average κ value (κ_{ccn}, 0.46 ± 0.02) derived from CCN activity measurement (Tang et al., 2019c). The growth factor was measured to be 1.53 ± 0.04 at 90% RH for CH_3SO_3K aerosol, and consequently κ_{gf} was determined to be 0.26–0.32, again significantly smaller than the κ_{ccn} value (0.47 ± 0.02) reported in a previous study (Tang et al., 2019c). For $(CH_3SO_3)_2Ca$ aerosol, the measured growth factor (1.65 ± 0.02) at 90% RH corresponded to κ_{gf} in the range of 0.36–0.40; two previous studies (Tang et al., 2015, 2019c) investigated CCN activity of $(CH_3SO_3)_2Ca$ aerosol, and κ_{ccn} values were reported to be 0.30–0.38 (Tang et al., 2015) and 0.37 ± 0.01 (Tang et al., 2019c), in good agreement with κ_{gf} derived in the present work.

Previous work (Petters and Kreidenweis, 2007; Petters et al., 2009; Wex et al., 2009; Hansen et al., 2015) found both good agreement and significant difference between κ_{gf} and κ_{ccn}, and the discrepancies could be attributed to several factors. As CH_3SO_3Na and CH_3SO_3K are both highly soluble, the difference between κ_{gf} and κ_{ccn} cannot be caused by solubility limit. The κ_{ccn} values of CH_3SO_3Na reported in previous work (Tang et al., 2019c) were calculated using surface tension of pure water; however, Liu et al. (2011) found that surface tension of CH_3SO_3Na solutions was significantly smaller than pure water. Therefore, we speculate that difference in surface tension between CH_3SO_3Na solutions and pure water may at least partly explain the discrepancies between κ_{gf} and κ_{ccn} for CH_3SO_3Na aerosol. Further experimental and theoretical studies are needed to better understand its hygroscopicity under sub- and super-saturated conditions.

4. Conclusions

In this work, hygroscopic properties of CH_3SO_3Na, CH_3SO_3K and $(CH_3SO_3)_2Ca$ were investigated using two experimental methods. The change in sample mass with RH was measured using a vapor sorption analyzer, and significant increase in sample mass was observed at >70% RH for all the three compounds. The mass growth factors, defined as the sample mass at a given RH to that under dry conditions, were determined to be 4.002 ± 0.053 for CH_3SO_3Na, 3.479 ± 0.031 for CH_3SO_3K, and 3.663 ± 0.019 for $(CH_3SO_3)_2Ca$ at 90% RH, respectively. In addition, DRH was measured to be 70–71% for CH_3SO_3Na at 15–35 °C, showing no dependence on temperature.

A humidity tandem differential mobility analyzer was employed to study hygroscopic growth of CH_3SO_3Na, CH_3SO_3K and $(CH_3SO_3)_2Ca$ aerosols. CH_3SO_3Na and CH_3SO_3K aerosols started to grow at >70%, while continuous hygroscopic growth was observed for $(CH_3SO_3)_2Ca$ aerosols even at very low RH (<40%). The growth factors were measured to be 1.48 ± 0.02, 1.53 ± 0.04 and 1.65 ± 0.02 for CH_3SO_3Na, CH_3SO_3K and $(CH_3SO_3)_2Ca$ aerosols at 90% RH, and thus the κ (the single hygroscopicity parameter) values were derived to be 0.24–0.26 for CH_3SO_3Na, 0.26–0.32 for CH_3SO_3K, and 0.36–0.40 for $(CH_3SO_3)_2Ca$. The κ values derived from hygroscopic growth and CCN activity measurements showed good agreements for $(CH_3SO_3)_2Ca$ aerosol but displayed large discrepancies for CH_3SO_3Na and CH_3SO_3K aerosols, and the discrepancy may result from lower surface tension of CH_3SO_3Na and CH_3SO_3K solutions, when compared to pure water.

Although methanesulfonate is an important component in marine aerosols, it has not been considered in widely used aerosol thermodynamic models such as E-AIM (Clegg et al., 1998) and ISORROPIA-II (Fountoukis and Nenes, 2007). In this work we systematically measured mass and diameter changes of CH_3SO_3Na, CH_3SO_3K and $(CH_3SO_3)_2Ca$ particles, and the comprehensive data obtained can be used to constrain aerosol thermodynamic models (when they are extended to include methanesulfonates) and verify their results.

Declaration of competing interest

The authors declare that they have no known competing financial interests or personal relationships that could have appeared to influence the work reported in this paper.

CRediT authorship contribution statement

Liya Guo: Formal analysis. **Chao Peng:** Formal analysis. **Taomou Zong:** Formal analysis. **Wenjun Gu:** Formal analysis. **Qingxin Ma:** Supervision. **Zhijun Wu:** Supervision. **Zhe Wang:** Supervision. **Xiang Ding:** Supervision. **Min Hu:** Supervision. **Xinming Wang:** Supervision. **Mingjin Tang:** Supervision, Formal analysis.

Acknowledgment

This work was funded by National Natural Science Foundation of China (91744204), State Key Laboratory of Organic Geochemistry (SKLOG2016-A05), Guangdong Province (2017GC010501) and Guangdong Foundation for Program of Science and Technology Research (2017B030314057). Mingjin Tang would like to thank the CAS Pioneer Hundred Talents program for providing a starting grant.

Appendix A. Supplementary data

Supplementary data to this article can be found online at https://doi.org/10.1016/j.atmosenv.2020.117349.

References

Andreae, M.O., 1990. Ocean-Atmosphere Interactions in the global biogeochemical sulfur cycle. Mar. Chem. 30, 1–29.
Bardouki, H., Berresheim, H., Vrekoussis, M., Sciare, J., Kouvarakis, G., Oikonomou, K., Schneider, J., Mihalopoulos, N., 2003. Gaseous (DMS, MSA, SO_2, H_2SO_4 and DMSO) and particulate (sulfate and methanesulfonate) sulfur species over the northeastern coast of Crete. Atmos. Chem. Phys. 3, 1871–1886.
Barnes, I., Hjorth, J., Mihalopoulos, N., 2006. Dimethyl sulfide and dimethyl sulfoxide and their oxidation in the atmosphere. Chem. Rev. 106, 940–975.
Bates, T.S., Calhoun, J.A., Quinn, P.K., 1992. Variations in the methanesulfonate to sulfate molar ratio in submicrometer marine aerosol particles over the south Pacific Ocean. J. Geophys. Res. 97, 9859–9865.
Bates, T.S., Kiene, R.P., Wolfe, G.V., Matrai, P.A., Chavez, F.P., Buck, K.R., Blomquist, B. W., Cuhel, R.L., 1994. The cycling of sulfur in surface seawater of the northeast Pacific. J. Geophys. Res. Oceans 99, 7835–7843.
Bertram, T.H., Cochran, R.E., Grassian, V.H., Stone, E.A., 2018. Sea spray aerosol chemical composition: elemental and molecular mimics for laboratory studies of heterogeneous and multiphase reactions. Chem. Soc. Rev. 47, 2374–2400.
Charlson, R.J., Lovelock, J.E., Andreae, M.O., Warren, S.G., 1987. Oceanic phytoplankton, atmospheric sulphur, cloud albedo and climate. Nature 326, 655–661.
Chen, H., Varner, M.E., Gerber, R.B., Finlayson-Pitts, B.J., 2016. Reactions of methanesulfonic acid with amines and ammonia as a source of new particles in air. J. Phys. Chem. B 120, 1526–1536.
Clegg, S.L., Brimblecombe, P., Wexler, A.S., 1998. Thermodynamic model of the system H^+-NH_4^+-Na^+-SO_4^{2-}-NO_3^--Cl^--H_2O at 298.15 K. J. Phys. Chem. 102, 2155–2171.
Davis, D., Chen, G., Bandy, A., Thornton, D., Eisele, F., Mauldin, L., Tanner, D., Lenschow, D., Fuelberg, H., Huebert, B., Heath, J., Clarke, A., Blake, D., 1999. Dimethyl sulfide oxidation in the equatorial Pacific: comparison of model simulations with field observations for DMS, SO_2, H_2SO_4(g), MSA(g), MS, and NSS. J. Geophys. Res. 104, 5765–5784.

Dawson, M.L., Varner, M.E., Perraud, V., Ezell, M.J., Gerber, R.B., Finlayson-Pitts, B.J., 2012. Simplified mechanism for new particle formation from methanesulfonic acid, amines, and water via experiments and ab initio calculations. Proc. Natl. Acad. Sci. U.S.A. 109, 18719–18724.

Debruyn, W.J., Shorter, J.A., Davidovits, P., Worsnop, D.R., Zahniser, M.S., Kolb, C.E., 1994. Uptake of gas phase sulfur species methanesulfonic acid, dimethylsulfoxide, and dimethyl sulfone by aqueous surfaces. J. Geophys. Res. 99, 16927–16932.

Eom, H.-J., Gupta, D., Li, X., Jung, H.-J., Kim, H., Ro, C.-U., 2014. Influence of collecting substrates on the characterization of hygroscopic properties of inorganic aerosol particles. Anal. Chem. 86, 2648–2656.

Fountoukis, C., Nenes, A., 2007. ISORROPIA II: a computationally efficient thermodynamic equilibrium model for K^+-Ca^{2+}-Mg^{2+}-NH_4^+-Na^+-SO_4^{2-}-NO_3^--Cl^--H_2O aerosols. Atmos. Chem. Phys. 7, 4639–4659.

Fuentes, E., Coe, H., Green, D., de Leeuw, G., McFiggans, G., 2010. Laboratory-generated primary marine aerosol via bubble-bursting and atomization. Atmos. Meas. Tech. 3, 141–162.

Gibson, E.R., Hudson, P.K., Grassian, V.H., 2006. Aerosol chemistry and climate: laboratory studies of the carbonate component of mineral dust and its reaction products. Geophys. Res. Lett. 33 https://doi.org/10.1029/2006GL026386.

Gondwe, M., Krol, M., Klaassen, W., Gieskes, W., de Baar, H., 2004. Comparison of modeled versus measured MSA : nss $SO_4^=$ ratios: a global analysis. Global Biogeochem. Cycles 18. https://doi.org/10.1029/2003GB002144.

Gu, W., Li, Y., Tang, M., Jia, X., Ding, X., Bi, X., Wang, X., 2017a. Water uptake and hygroscopicity of perchlorates and implications for the existence of liquid water in some hyperarid environments. RSC Adv. 7, 46866–46873.

Gu, W., Li, Y., Zhu, J., Jia, X., Lin, Q., Zhang, G., Ding, X., Song, W., Bi, X., Wang, X., Tang, M., 2017b. Investigation of water adsorption and hygroscopicity of atmospherically relevant particles using a commercial vapor sorption analyzer. Atmos. Meas. Tech. 10, 3821–3832.

Guo, L., Gu, W., Peng, C., Wang, W., Li, Y.J., Zong, T., Tang, Y., Wu, Z., Lin, Q., Ge, M., Zhang, G., Hu, M., Bi, X., Wang, X., Tang, M., 2019. A comprehensive study of hygroscopic properties of calcium- and magnesium-containing salts: implication for hygroscopicity of mineral dust and sea salt aerosols. Atmos. Chem. Phys. 19, 2115–2133.

Gupta, D., Eom, H.J., Cho, H.R., Ro, C.U., 2015. Hygroscopic behavior of NaCl-$MgCl_2$ mixture particles as nascent sea-spray aerosol surrogates and observation of efflorescence during humidification. Atmos. Chem. Phys. 15, 11273–11290.

Hansen, A.M.K., Hong, J., Raatikainen, T., Kristensen, K., Ylisirnio, A., Virtanen, A., Petaja, T., Glasius, M., Prisle, N.L., 2015. Hygroscopic properties and cloud condensation nuclei activation of limonene-derived organosulfates and their mixtures with ammonium sulfate. Atmos. Chem. Phys. 15, 14071–14089.

Hanson, D.R., 2005. Mass accommodation of H_2SO_4 and CH_3SO_3H on water-sulfuric acid solutions from 6% to 97% RH. J. Phys. Chem. 109, 6919–6927.

Haywood, J., Boucher, O., 2000. Estimates of the direct and indirect radiative forcing due to tropospheric aerosols: a review. Rev. Geophys. 38, 513–543.

Hodshire, A.L., Campuzano-Jost, P., Kodros, J.K., Croft, B., Nault, B.A., Schroder, J.C., Jimenez, J.L., Pierce, J.R., 2019. The potential role of methanesulfonic acid (MSA) in aerosol formation and growth and the associated radiative forcings. Atmos. Chem. Phys. 19, 3137–3160.

Huang, S., Poulain, L., van Pinxteren, D., van Pinxteren, M., Wu, Z., Herrmann, H., Wiedensohler, A., 2017. Latitudinal and seasonal distribution of particulate MSA over the Atlantic using a validated quantification method with HR-ToF-AMS. Environ. Sci. Technol. 51, 418–426.

Jia, X., Gu, W., Li, Y.J., Cheng, P., Tang, Y., Guo, L., Wang, X., Tang, M., 2018. Phase transitions and hygroscopic growth of $Mg(ClO_4)_2$, $NaClO_4$, and $NaClO_4{\cdot}H_2O$: implications for the stability of aqueous water in hyperarid environments on Mars and on Earth. ACS Earth Space Chem. 2, 159–167.

Jing, B., Wang, Z., Tan, F., Guo, Y., Tong, S., Wang, W., Zhang, Y., Ge, M., 2018. Hygroscopic behavior of atmospheric aerosols containing nitrate salts and water-soluble organic acids. Atmos. Chem. Phys. 18, 5115–5127.

Kanakidou, M., Seinfeld, J., Pandis, S., Barnes, I., Dentener, F., Facchini, M., Dingenen, R. V., Ervens, B., Nenes, A., Nielsen, C., 2005. Organic aerosol and global climate modelling: a review. Atmos. Chem. Phys. 5, 1053–1123.

Kelly, W.P., McMurry, P.H., 1992. Measurement of particle density by inertial classification of differential mobility analyzer–generated monodisperse aerosols. Aerosol Sci. Technol. 17, 199–212.

Kwong, K.C., Chim, M.M., Hoffmann, E.H., Tilgner, A., Herrmann, H., Davies, J.F., Wilson, K.R., Chan, M.N., 2018. Chemical transformation of methanesulfonic acid and sodium methanesulfonate through heterogeneous OH oxidation. ACS Earth Space Chem. 2, 895–903.

Laskina, O., Morris, H.S., Grandquist, J.R., Qin, Z., Stone, E.A., Tivanski, A.V., Grassian, V.H., 2015. Size matters in the water uptake and hygroscopic growth of atmospherically relevant multicomponent aerosol particles. J. Phys. Chem. 119, 4489–4497.

Lin, C.T., Baker, A.R., Jickells, T.D., Kelly, S., Lesworth, T., 2012. An assessment of the significance of sulphate sources over the Atlantic Ocean based on sulphur isotope data. Atmos. Environ. 62, 615–621.

Liu, Y., Laskin, A., 2009. Hygroscopic properties of CH_3SO_3Na, $CH_3SO_3NH_4$, $(CH_3SO_3)_2Mg$, and $(CH_3SO_3)_2Ca$ particles studied by micro-FTIR spectroscopy. J. Phys. Chem. 113, 1531–1538.

Liu, Y., Minofar, B., Desyaterik, Y., Dames, E., Zhu, Z., Cain, J.P., Hopkins, R.J., Gilles, M. K., Wang, H., Jungwirth, P., Laskin, A., 2011. Internal structure, hygroscopic and reactive properties of mixed sodium methanesulfonate-sodium chloride particles. Phys. Chem. Chem. Phys. 13, 11846–11857.

Ma, Q., Zhong, C., Liu, C., Liu, J., Ma, J., Wu, L., He, H., 2019. A Comprehensive study about the hygroscopic behavior of mixtures of oxalic acid and nitrate salts: implication for the occurrence of atmospheric metal oxalate complex. ACS Earth Space Chem. 3, 1216–1225.

Mungall, E.L., Wong, J.P.S., Abbatt, J.P.D., 2018. Heterogeneous oxidation of particulate methanesulfonic acid by the hydroxyl radical: kinetics and atmospheric implications. ACS Earth Space Chem. 2, 48–55.

Ovadnevaite, J., Ceburnis, D., Leinert, S., Dall'Osto, M., Canagaratna, M., O'Doherty, S., Berresheim, H., O'Dowd, C., 2014. Submicron NE Atlantic marine aerosol chemical composition and abundance: seasonal trends and air mass categorization. J. Geophys. Res. 119, 11850–11863.

Peng, C.G., Chan, C.K., 2001. The water cycles of water-soluble organic salts of atmospheric importance. Atmos. Environ. 35, 1183–1192.

Petters, M.D., Kreidenweis, S.M., 2007. A single parameter representation of hygroscopic growth and cloud condensation nucleus activity. Atmos. Chem. Phys. 7, 1961–1971.

Petters, M.D., Wex, H., Carrico, C.M., Hallbauer, E., Massling, A., McMeeking, G.R., Poulain, L., Wu, Z., Kreidenweis, S.M., Stratmann, F., 2009. Towards closing the gap between hygroscopic growth and activation for secondary organic aerosol - Part 2: theoretical approaches. Atmos. Chem. Phys. 9, 3999–4009.

Sorooshian, A., Crosbie, E., Maudlin, L.C., Youn, J.-S., Wang, Z., Shingler, T., Ortega, A. M., Hersey, S., Woods, R.K., 2015. Surface and airborne measurements of organosulfur and methanesulfonate over the western United States and coastal areas. J. Geophys. Res. 120, 8535–8548.

Tang, M., Zhu, T., 2008. Heterogeneous reactions of gaseous methanesulfonic acid with NaCl and sea salt particles. Sci. China, Ser. B: Inside Chem. 52, 93–100.

Tang, M., Li, M., Zhu, T., 2010. Heterogeneous reactions of gaseous methanesulfonic acid with calcium carbonate and kaolinite particles. Sci. China Chem. 53, 2657–2662.

Tang, M., Cziczo, D.J., Grassian, V.H., 2016. Interactions of water with mineral dust aerosol: water adsorption, hygroscopicity, cloud condensation, and ice nucleation. Chem. Rev. 7, 4205–4259.

Tang, M., Chan, C.K., Li, Y.J., Su, H., Ma, Q., Wu, Z., Zhang, G., Wang, Z., Ge, M., Hu, M., He, H., Wang, X., 2019a. A review of experimental techniques for aerosol hygroscopicity studies. Atmos. Chem. Phys. Discuss. 1–130. https://doi.org/10.5194/acp-2019-398.

Tang, M., Gu, W., Ma, Q., Li, Y.J., Zhong, C., Li, S., Yin, X., Huang, R.-J., He, H., Wang, X., 2019b. Water adsorption and hygroscopic growth of six anemophilous pollen species: the effect of temperature. Atmos. Chem. Phys. 19, 2247–2258.

Tang, M., Guo, L., Bai, Y., Huang, R.-J., Wu, Z., Wang, Z., Zhang, G., Ding, X., Hu, M., Wang, X., 2019c. Impacts of methanesulfonate on the cloud condensation nucleation activity of sea salt aerosol. Atmos. Environ. 201, 13–17.

Tang, M.J., Whitehead, J., Davidson, N.M., Pope, F.D., Alfarra, M.R., McFiggans, G., Kalberer, M., 2015. Cloud condensation nucleation activities of calcium carbonate and its atmospheric ageing products. Phys. Chem. Chem. Phys. 17, 32194–32203.

van Pinxteren, M., Fiedler, B., van Pinxteren, D., Iinuma, Y., Koertzinger, A., Herrmann, H., 2015. Chemical characterization of sub-micrometer aerosol particles in the tropical Atlantic Ocean: marine and biomass burning influences. J. Atmos. Chem. 72, 105–125.

Wex, H., Petters, M.D., Carrico, C.M., Hallbauer, E., Massling, A., McMeeking, G.R., Poulain, L., Wu, Z., Kreidenweis, S.M., Stratmann, F., 2009. Towards closing the gap between hygroscopic growth and activation for secondary organic aerosol: Part 1-Evidence from measurements. Atmos. Chem. Phys. 9, 3987–3997.

Wexler, A.S., Clegg, S.L., 2002. Atmospheric aerosol models for systems including the ions H^+, NH_4^+, Na^+, SO_4^{2-}, NO_3^-,Cl^-, Br^-, and H_2O. J. Geophys. Res. 107, D14. https://doi.org/10.1029/2001JD000451.

Wu, Z., Zheng, J., Wang, Y., Shang, D., Du, Z., Zhang, Y., Hu, M., 2017. Chemical and physical properties of biomass burning aerosols and their CCN activity: a case study in Beijing, China. Sci. Total Environ. 579, 1260–1268.

Wu, Z.J., Nowak, A., Poulain, L., Herrmann, H., Wiedensohler, A., 2011. Hygroscopic behavior of atmospherically relevant water-soluble carboxylic salts and their influence on the water uptake of ammonium sulfate. Atmos. Chem. Phys. 11, 12617–12626.

Zeng, G., Kelley, J., Kish, J.D., Liu, Y., 2014. Temperature-dependent deliquescent and efflorescent properties of methanesulfonate sodium studied by ATR-FTIR spectroscopy. J. Phys. Chem. 118, 583–591.

Zhao, H., Jiang, X., Du, L., 2017. Contribution of methane sulfonic acid to new particle formation in the atmosphere. Chemosphere 174, 689–699.

Zieger, P., Vaisanen, O., Corbin, J.C., Partridge, D.G., Bastelberger, S., Mousavi-Fard, M., Rosati, B., Gysel, M., Krieger, U.K., Leck, C., Nenes, A., Riipinen, I., Virtanen, A., Salter, M.E., 2017. Revising the hygroscopicity of inorganic sea salt particles. Nat. Commun. 8, 15883 https://doi.org/10.1038/ncomms15883.

Zorn, S.R., Drewnick, F., Schott, M., Hoffmann, T., Borrmann, S., 2008. Characterization of the South Atlantic marine boundary layer aerosol using an aerodyne aerosol mass spectrometer. Atmos. Chem. Phys. 8, 4711–4728.